Chapter 8

A critical evaluation of the relevant parameters for drug redispersion from adhesive mixtures during inhalation

A.H. de Boer[1], B.H.J. Dickhoff[2], P. Hagedoorn[1], D. Gjaltema[1], J. Goede[3], D. Lambregts[4], H.W. Frijlink[1]

[1]Department of Pharmaceutical Technology and Biopharmacy, Groningen University Institute for Drug Exploration (GUIDE), Ant. Deusinglaan 1, 9713 AV Groningen, The Netherlands.
[2]Inhalation and Product Development (IPD), GSK R&D, Ware, UK.
[3]Sofotec GmbH&CoKG, Benzstrasse 1, D-61352 Bad Homburg, Germany.
[4]DMV International, P.O. Box 13, 5460 BA Veghel, The Netherlands.

Published in Int. J. Pharm. 294 92005) 173-184.

Abstract

The parameters that are relevant to the drug redispersion from adhesive mixtures during inhalation are discussed and evaluated. The results obtained with air classifier technology give strong evidence for a dominating influence of carrier surface properties on the fraction of drug detached during inhalation at a low carrier payload (≤ 1% w/w), versus a dominating effect of carrier bulk properties at higher payloads. Furthermore, the results indicate that there is a fundamental difference between so-called active carrier sites and large surface discontinuities. The difference refers to the saturation concentrations, the rates of saturation and their effects on drug detachment during inhalation. The degree of saturation of the active sites appears to be proportional with the square root of the carrier surface payload (after 10 min mixing time in a Turbula mixer at 90 rpm). The storage volume of the discontinuities seems largely independent of the carrier diameter for particles derived from the same batch of crystalline lactose. Saturation of these discontinuities is completed at a much lower carrier surface payload than saturation of the active sites. Relatively large discontinuities are beneficial to de-agglomeration principles that make use of inertial separation forces during inhalation, as they provide shelter from inertial and frictional press-on forces during mixing which increase the strength of the interparticulate bonds in the powder mixture. For de-agglomeration principles generating frictional, drag or lift forces, carrier surface depressions and projections are disadvantageous however, as they also provide shelter from these removal forces.

Key words: Active sites, Adhesive mixtures, Carrier payload, Carrier size, Large carrier surface discontinuities, Press-on forces

1. Introduction

Existing theories for adhesive mixtures for inhalation take the view that active carrier sites and carrier rugosity play dominant roles in the interaction between the drug and carrier particles. It has been found that a large number of active sites and a high rugosity reduce the fraction of drug detached during inhalation (Ganderton and Kassem, 1991; Kawashima et al., 1998), and the carrier rugosity has been considered as an appearance of active sites (e.g. Staniforth, 1995, 1996). These findings and conceptions are understandable, as drug to carrier ratios in adhesive mixtures for inhalation are often 1: 67.5 (1.46% w/w drug; e.g. Larhrib et al., 1999; Zeng et al., 2000; Flament et al., 2004), whereas the carriers for these mixtures mostly have a size range smaller than 100 µm (e.g. Kawashima et al., 1998; Larhrib et al., 1999; Flament et al., 2004). This combination of conditions results in relatively low carrier surface payloads, meaning that there may be many carrier sites with high bonding energy or surface discontinuities relative to the number of drug particles on the carrier surface. Additionally, inhalers generating drag, lift or friction forces have been used for drug redispersion in most studies. These types of detachment forces are not very effective in separating drug particles from carrier surface irregularies during inhalation.

The conditions may be selected differently however. Much higher as well as much lower carrier payloads may be desired, or necessary for new inhalation drugs (e.g. Schlimmer, 2000; Newhouse et al., 2003). Coarser carrier fractions may be used, which yield a much better dose emission from the inhaler (Staniforth, 1995; Zeng et al., 2001b), although the use of such fractions introduces a new variable, which is the action of inertial and frictional (press-on) forces during mixing. These press-on forces may increase the interparticulate forces in the powder and their magnitude increases with the mean carrier diameter (Dickhoff et al., 2003). Large carrier particles normally exhibit also larger surface discontinuities than fine crystals (de Boer et al., 2003b). This may have the advantage of providing shelter to drug particles from the press-on forces during mixing, as the drug particles tend to assemble in these discontinuities during mixing (Kulvanich and Stewart, 1987; Iida et al., 2003). Therefore, a high carrier rugosity does not necessarily have a negative effect on the drug detachment from carrier crystals during inhalation, providing that inertial detachment forces are applied (e.g. Dickhoff et al., 2005a). Having an advantage from the use of high carrier rugosities depends also on the size and volume of the carrier surface discontinuities in relation to the carrier payload and the mixing conditions (e.g. Dickhoff et al., 2003, 2005b). If the drug amount in the mixture is higher than can be stored in the carrier discontinuities, the fraction of drug detached from the carrier crystals generally decreases with increasing carrier size (equals increasing magnitude of the press-on forces).

The aim of this study is a critical evaluation of the parameters that influence the drug-to-carrier interaction during mixing and drug detachment during inhalation respectively. To make this evaluation meaningful, it has been assessed which fraction of the drug in the powder mixture can be attached to active carrier sites, or be stored in the carrier surface discontinuities respectively. The relevance of both aspects is discussed in relation to the powder bulk properties and the mixing procedure (which both influence the press-on forces during mixing) and the inhalation conditions (referring to the type and magnitude of the generated detachment forces). Findings and conclusions from previous classifier studies, as well as results of some new investigations have been used to support the discussions.

2. Materials and methods

2.1. Materials

Carrier size fractions were derived from Pharmatose 80, 100, 150 and 200 M (DMV International, Veghel, The Netherlands). Different micronised budesonide samples were used for the study. They were supplied by Sofotec (Frankfurt, Germany) and their volume median diameters (from laser diffraction analysis) were 1.04; 1.32, 1.35 and 1.46 μm respectively.

2.2. Preparation and characterisation of carrier fractions and adhesive mixtures

Carrier fractions of different size ranges were obtained by sieving small batches (approx. 100 g) of lactose for 20 min on a vibratory sieving machine (Analysette, 3, Fritsch, Germany) followed by 20 min on an air jet sieve (A200, Alpine, Germany) to remove adhering fines. All fractions were investigated with laser diffraction technique (Sympatec HELOS BF-MAGIC, Germany) and scanning electron microscopy (JEOL JSM 6301-F, Japan) prior to mixture preparation. For laser diffraction analysis, the fractions were dispersed with a RODOS disperser at 3 or 5 bar. A 100, 200 or 500 mm lens was applied and calculations were made with the Fraunhofer theory. For SEM investigation, powder samples were sprinkled on double-sided sticky tape (on metal disks) and coated with 150 nm of gold/palladium in a sputtering device (Balzers 120B, Liechtenstein).

Mixtures were prepared in batch sizes of 25 g, using a special stainless steel mixing container of 160 x 10^{-6} m^3. Mixing time was 10 min (unless stated otherwise) in a tumbling mixer operated at 90 rpm (Turbula T2C, WA Bachofen, Switzerland). Inhalation experiments were not undertaken within less than a week after mixture preparation. Mixture homogeneity was tested on 20 samples of 25 mg taken randomly from the powder. The samples were dissolved in 15-20 ml of pure ethanol and the solutions were separated from non-dissolved lactose crystals in a centrifuge during 5 min at 3000 rpm (Rotana 3500, Hettich, Germany) prior to spectrophotometrical analysis at 242.8 nm (Philips PU 8720 UV-VIS, The Netherlands).

2.3. Carrier residue measurements

For the carrier residue measurements, a previously described test inhaler with basic air classifier was used (de Boer et al., 2003a). The metal inhaler was earthed during the experiments to avoid tribocharge and either connected to a single impinger or to a multi stage impactor and the flow curve through the inhaler was adjusted to be 30 or 60 l/min (3 s) with a flow control system including a 3-way valve connected to a timer. The inhaler was loaded manually with 25 mg powder mixture before each experiment to exclude variations from poor dosing accuracy. After each test, retained carrier particles were collected from the classifier and analysed upon residual drug, using the procedures described for homogeneity testing of the mixtures. Each data point is the mean of two series of 5 to 10 inhalations.

2.4. Calculations and definitions

The terms and definitions used in this chapter to explain the performance of adhesive mixtures in an air classifier are summarized in Table 8.1. Additionally, the percent of drug detached from carrier equals 100 minus carrier residue (CR).

Carrier surface payload (CSP in g/m^2) is the ratio of the carrier payload (in g/g) to the calculated specific surface area of the carrier fraction (in m^2/g). The specific surface area (S_g) is based on the arithmetic mean diameter (D) of the size fraction ($S_g = 6D^{-1}.\rho^{-1}$), where ρ is the density of α-lactose monohydrate (1.54 x 10^6 g/m^3).

Table 8.1. Summary of terms and definitions.

Term	Definition
Carrier payload	Weight fraction of drug in the mixture (% w/w)
Carrier surface payload (CSP)	Weight load of drug per unit carrier surface area (g/m^2)
(Initial) Carrier coverage (CC)	Carrier surface payload as percent of a monolayer of drug particles around the carrier crystals (see materials and methods: calculations)
Carrier retention	Amount of carrier particles retained in the classifier during inhalation (as percent of carrier weight in the dose)
Carrier residue (CR)	Residual drug on retained carrier crystals after inhalation as percent of the initial payload (and corrected for 100% retention)
Residual carrier (surface) payload	Carrier surface payload after inhalation (g/m^2)

For computation of the percent theoretical carrier coverage (CC), it was assumed that drug particles are spherical and monodisperse (the diameter equals X_{50} from laser diffraction analysis, dry dispersion with RODOS a 5 bar). It was furthermore assumed that the projection area of a single drug particle on the carrier surface equals the square of its diameter. From the carrier payload (g/g) and the drug particle weight ($W = V.\rho = \pi.d^3.\rho/6$, where ρ is the density of budesonide: 1.24×10^6 g/m^3), the number of drug particles on the carrier surface could be calculated. The number multiplied by the projection area of a single particle yielded the total projection area (in m^2/m^2) and multiplication of the projection area by 100, the percent theoretical CC. It should be clear that computed CC has only an indicative value which enables to differentiate between the fractions of carrier surface that could theoretically be covered by drug particles when different carrier size fractions are mixed with the same amount of drug (% w/w). Real CC will depend on many factors, including the degree of drug agglomeration on the carrier surface.

To obtain a better understanding of the degree of saturation of the active sites at different drug concentrations in the mixture (obtained after 10 min mixing time), the payload of these sites as function of the carrier payload was modelled. Computations were made for a coarse carrier fraction (250-355 μm) and the computed data were compared with the experimentally obtained data for this fraction (Fig. 8.5), which showed that saturation is complete (0.144 g/m^2) when the carrier surface payload is 3.1 g/m^2 (Table 8.2).

Three different computations were made, assuming respectively:

1. that all drug particles in the mixture are exclusively attached to the active sites, unless the drug amount in the mixture is higher than the saturation payload (storage capacity) of these sites, in which case the excess of drug particles is spread over the remaining carrier surface (referred to in Fig. 8.5 as ‘maximal increase’),
2. that the payload of the active sites increases proportionally with the drug amount in the mixture (‘proportional increase’), and
3. that the payload of the active sites (AP) increases exponentially with the drug amount in the mixture (expressed as carrier surface payload: CSP; ‘exponential increase’).

Of these three different calculations, the exponential increase turned out to give the best fit with the experimental results for 10 min mixing time when using a square root function ($CSP^{0.5} = C.AP$). In this equation, the constant C (obtained from substitution of AP and CSP in the saturation situation) equals 12.227. The fraction of drug detached has been calculated as CSP minus corresponding AP, and this fraction has been expressed as percent of CSP, for increment steps of 0.1CSP.

3. Results and discussion

3.1. The binding capacity of active sites

Fig. 8.1 summarises the results from various experiments with the same classifier based test inhaler for adhesive mixtures with crystalline carrier fractions. In this figure, the residual carrier surface payload (in g/m^2) is presented as function of the initial carrier payload (in % w/w) for experiments performed at 30 and 60 l/min.

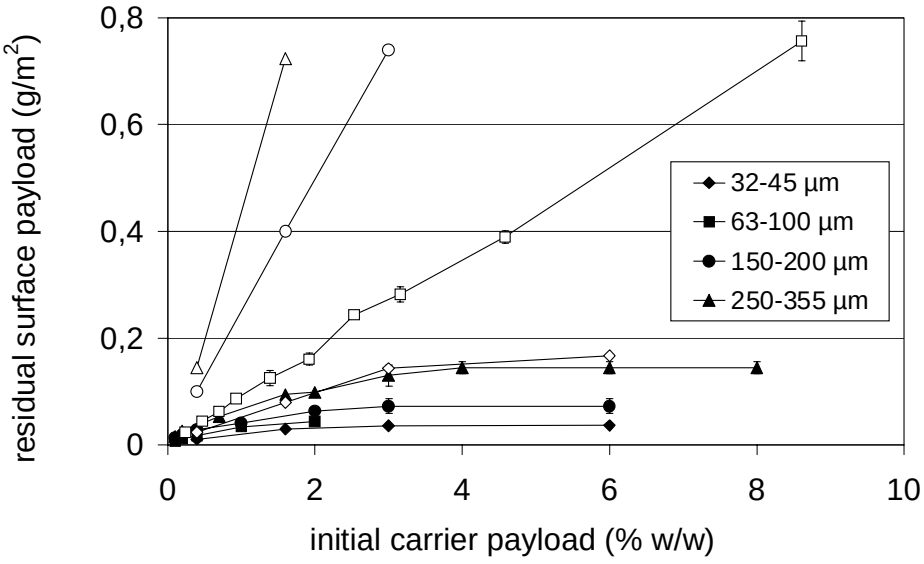

Figure 8.1. Residual carrier surface payload (g/m^2) as function of initial payload (% w/w) at 30 l/min (open symbols) and 60 l/min (closed symbols) respectively: 3 s inhalation time. The spread bars shown for the 63-106 µm fraction at 30 l/min indicate maximal and minimal values obtained and are indicative for the variations found with other carrier size fractions. At 60 l/min, spread bars are given for all fractions.

The relationships at 30 l/min confirm the findings of Dickhoff et al. (2003). They showed that increasing the mean carrier diameter results in higher binding forces between the drug and carrier particles in the powder mixture at higher carrier payloads. As a consequence, a higher residual surface payload (at the same initial carrier payload) after inhalation (at 30 l/min) is obtained. This has been explained with higher press-on forces during mixing for coarser carrier fractions, of which the effect becomes particularly noticeable at higher carrier payloads.

At 60 l/min, the ratio of (mean) removal forces (F_R) in a classifier to the adhesive forces (F_A) in the mixture is so high, that only a minor fraction of the drug can not be detached. At this high flow rate, all three residual carrier surface payloads reach a constant value at higher initial payloads. This constant value is highest (0.144 g/m^2) for the coarsest fraction, having also the highest degree of surface impurities and irregularities (de Boer et al., 2003b) and lowest (0.035 g/m^2) for the finest fraction. The constant values at higher payload seem to point in the direction of a saturation of the carrier sites with the strongest bonding forces (active sites). Surprisingly, saturation is first complete at a relatively high initial carrier payload of approximately 3 to 4% (w/w). This payload corresponds with a carrier surface payload of 0.3 g/m^2 for carrier fraction 32-45 µm and 3.1 g/m^2 for the size fraction 250-355 µm respectively, as shown in Table 8.2. The numerical values for the saturation payloads for

the active sites derived from Fig. 8.1 indicate only the order of magnitude for the carriers used. As already mentioned, they depend on the applied ratio of removal to adhesive forces. They may be different for different types of lactose, whereas also batch variations for the same type of lactose may occur. This has been explained previously (de Boer et al., 2003b).

Table 8.2. Estimated saturation concentrations for active sites and large surface discontinuities of different carrier size fractions and the carrier payloads at which saturation is achieved. Data derived from Figs. 8.1 and 8.2.

Fraction	Active sites				Large surface discontinuities		
(μm)	Saturation conc.	Saturation achieved at			Saturation concentration achieved at		
	g/m^2	% w/w	g/m^2	% CC	% w/w	g/m^2	% CC
32-45	0.0353	3	0.297	34	-	-	-
150-200 min	-	-	-	-	0.2	0.091	10
150-200 max	0.0723	3	1.357	155	1	0.452	52
250-355 min	0.1300	3	2.356	269	0.2	0.155	18
250-355 max	0.1440	4	3.100	354	1	0.775	88

% CC computed for budesonide with mean diameter of 1.35 μm

3.2. The storage capacity of large surface discontinuities

As already mentioned in the introduction, carrier surface discontinuities like pores and clefts or the steep faces of surface projections are places where drug particles can find shelter from inertial and frictional press-on forces during mixing (de Boer et al., 2003a; Dickhoff et al., 2003, 2005a). They are also places where drag, lift and friction types of removal force can not effectively get hold of the drug particles during inhalation. So, whether a high carrier rugosity is an advantage or not, depends on the type of inhaler used. Fig. 8.2 shows relationships between the percent of drug detached and the initial percent of carrier payload for different carrier size fractions at 30 l/min. As expected on the basis of previous experiments, percent detached initially increases with increasing payload for all carrier fractions (Dickhoff et al., 2003). This has been explained with an increasing excess of drug particles relative to the number of active sites.

At higher payloads, percent detached for coarse carrier fractions may either reach a maximum first and decrease next (coarse carrier I), or become constant immediately following a much lower initial increase (coarse carrier II). For both types of coarse carrier, percent detached at payloads above 4% (w/w) is approximately the same however. Therefore, Fig. 8.2 partially shades a previously drawn conclusion that the percent CR continues to increase for coarse carriers when the carrier payload is increased (Dickhoff et al., 2003). When the results from several studies (with different carrier batches) are averaged, the conclusion is rather that the percent of drug detached from coarse carrier crystals reaches a constant (plateau) value at high carrier payloads (as for intermediate carriers).

The difference between both coarse carrier fractions (I and II) could be the result of differences in the size distribution or agglomeration tendency of the drug, as different batches of budesonide have been used for different experiment series in Fig. 8.2. On the other hand, it could also be a difference in carrier properties. Investigation of coarse carrier fractions derived from different lactose batches of the same type also revealed that the mass fraction of adhering fines (< 5 μm) may vary from nearly zero to more than one percent (for the classification procedures used). Because fine lactose particles may be wiped into the large carrier surface discontinuities during mixing too, their presence could shift the saturation concentration of these discontinuities towards lower carrier payloads. This particular role of lactose fines in the mixture will be further investigated.

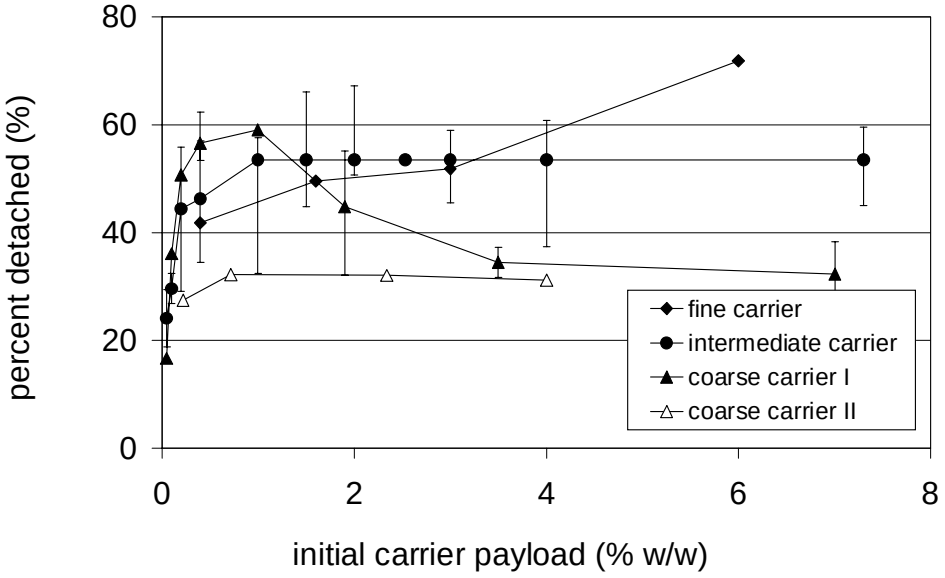

Figure 8.2. Percent of drug detached from carrier as function of initial percent carrier payload (% w/w). Fraction 32-45 µm has been considered as fine carrier; fractions 45-63; 63-90; 63-106 and 150-200 µm as intermediate, and fraction 250-355 as coarse carrier. Coarse I and coarse II are explained in the text.

The relationship for the intermediate fraction in Fig. 8.2 is the mean of different carrier fractions ranging from 45-63 to 150-200 µm. The plateau values are approximately 30% for coarse, and between 40 and 60% for intermediate fractions respectively. The highest payload of 6% in Fig. 8.2 of the finest fraction (32-45 µm) corresponds with a theoretical degree of carrier coverage of only 67% (for budesonide with a median diameter of 1.35 µm) and this appeared to be insufficient to reach a plateau. On the other hand, there may not be a plateau for fine carriers, as their mixtures with drug may behave differently in various respects, as will be explained in Paragraph 3.5 of this Chapter.

Reaching a maximum or a constant level in percent detached at 30 l/min when the carrier payload is increased, indicates a change in conditions which could be another saturation (as in Fig. 8.1). Fig. 8.2 shows that the peak or plateau value for percent detached (for coarse and intermediate carrier fractions) is obtained at a carrier payload of approximately 1% (w/w). For the budesonide particles used, a payload of 1% corresponds with (theoretical) degrees of carrier coverage of 52% for a carrier fraction 150-200 µm, and 88% for a fraction 250-355 µm respectively. This is considerably less than found necessary for the saturation of the active sites (155 and 354%, derived from Fig. 8.1: see Table 8.2). Considering furthermore that the results in Fig. 8.2 have been obtained at a lower flow rate (compared to Fig. 8.1), and that the ratio of removal forces to adhesive forces has thus been lower, the change in conditions in Fig. 8.2 seems to have no relationship with active sites at all. Neither seems a change from predominantly adhesive to cohesive forces in the mixture responsible for the constant values at high carrier payload, as this change would occur first at a carrier coverage of 100% (or more). Moreover, in that case there would be no reason for a difference in the percent detached between intermediate and coarse carrier fractions at higher payload. Particularly this difference points in the direction of an effect of the press-on forces, which can be explained with saturation of the large carrier surface discontinuities. The

observation that drug particles have a preference for gathering in the carrier surface cavities during mixing supports this explanation (Kulvanich and Stewart, 1987; Iida et al., 2003). Before saturation, the percent drug detached from the carrier crystals increases with increasing payload due to an increasing excess of drug particles to carrier sites with high bonding places. But as soon as the carrier discontinuities get filled up, drug particles are bound to spread over the remaining carrier surface. At this point they become in reach of the inertial and frictional (press-on) forces during mixing which increase the interparticulate forces in the powder, and the increase is highest for the coarsest carrier particles. As a result, a more or less constant fraction of the drug mass around the carrier particles is worn away during 3 s of circulation in a classifier at the relatively low flow rate of 30 l/min. The size of this fraction seems to be dependent on the magnitude of the (press-on) forces with which the carrier particles were kneaded around the carrier particles.

Although saturation of the carrier surface discontinuities is more or less complete at 1% payload, the initially high increase rate in percent dislodged already starts to fall off at approximately 0.2% payload (for all carrier fractions in Fig. 8.2). Apparently, spreading of drug particles over the remaining carrier surface starts already when the carrier surface discontinuities are only partially filled. At this payload of 0.2% the powder in the carrier discontinuities is likely to have an extremely high porosity, which is decreased at higher payload by the action of the inertial and frictional press-on forces during mixing also. The carrier surface payloads and degrees of carrier coverage corresponding with 0.2 and 1% payload for the carrier fractions 150-200 and 250-355 μm are given in Table 8.2.

3.3. The effect of mixing time

The rather high initial carrier payload (approx. 3%) that seems necessary to achieve saturation of the active carrier sites (Table 2) indicates that drug particles are distributed over both active and less active carrier sites initially (i.e. after short mixing times). This explains why increasing the mixing time at low carrier payloads has such a great effect on CR, as shown in Fig. 8.3. In this figure, the fraction of drug detached from mixtures prepared with 60 min mixing time is expressed as percent of the fraction detached from mixtures prepared with 10 min mixing. During mixing, drug particles subjected to relatively low adhesive forces may be detached from the carrier particles again and be relocated into areas with higher bonding capacity. As a result of that, the number of particles attached to active sites increases with increasing mixing time and so, the percent of drug detached during inhalation is reduced.

At a high payload, when the excess of drug particles relative to the number of active sites is much greater, initial occupation of these sites (after short mixing times) is much higher, and there is less potential left for drug particle relocation. At a high payload, also the carrier surface discontinuities may be saturated, meaning that inertial and frictional press-on forces can increase the adhesive forces of particles attached to sites with lower bonding capacity. So, not only the relocation potential but also its propensity is reduced. The increase in the adhesive forces by the action of the press-on forces may be quite substantial (Fig. 8.2), but the increase appears to decline exponentially with the mixing time (Dickhoff et al., 2003; de Boer et al., 2004a). For coarse carriers (with a high payload), a sub-maximal increase is already obtained after 10 min mixing time. For fine carriers, the effect of press-on forces is hardly noticeable (at 30 l/min). Therefore, the effect of mixing time between 10 and 60 min decreases with increasing carrier payload for all carrier size fractions. Table 8.3 shows that long mixing times are not always necessary. Already after 5 min, a good homogeneity may be obtained. Increasing the mixing time to 60 min reduces the percent drug detached for 0.4% mixtures with more than 30%, but it does not improve RSD significantly.

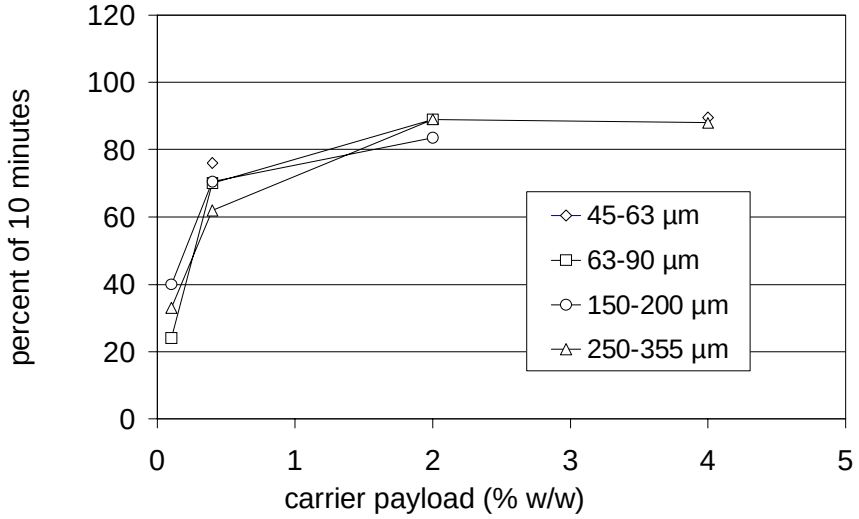

Figure 8.3. Percent of drug detached from carrier after 60 min mixing time as percent of that after 10 min mixing (at 30 l/min; 3 s), as function of carrier payload. Data from different studies with the same classifier using different budesonide samples and different carrier size fractions derived from Pharmatose 150 and 80 M.

Table 8.3. Comparison of the percent drug detached from carrier during inhalation at 30 l/min and mixture homogeneity (RSD), both as function of the mixing time for a mixture with carrier size fraction 63-106 µm and 0.4% (w/w) budesonide. Two similar carrier fractions were derived from Pharmatose 100M and 200M respectively.

Mixing time (min)	5	10	20	30	60
% detached 100M	56.1	55	49.9	47.9	40.5
RSD 100M (%)	2.57	1.5	2.23	2.87	1.71
% detached 200M	59.7	51.5	46.3	43	38.3
RSD 200M (%)	3.09	3.58	1.41	2.36	0.92

3.4. Summarising and evaluating the relevant parameters

The results in the Figs 8.1 to 8.3 prove that at least five different parameters are particularly relevant to the drug-to-carrier interaction during mixing and drug redispersion during inhalation:

1. the binding capacity and degree of saturation of the active carrier sites (in g/m^2), possibly including smaller carrier surface discontinuities, in respect of drug particle adhesion with high interparticulate forces,
2. the storage capacity of the large carrier surface discontinuities (in m^3/g), providing drug particles shelter from press-on forces during mixing (and certain types of detachment force during inhalation),
3. the magnitude and effectiveness of the press-on forces during mixing,
4. the intensity and duration of the mixing process, and
5. the type (and magnitude) of the detachment forces generated during inhalation.

Possible definitions for high carrier surface energy sites (active sites) have been discussed extensively in the past (e.g. Staniforth 1995; Buckton, 1997; de Boer et al., 2003b). In this chapter, active sites are simply defined as the sites from which drug particles are not detached at 60 l/min through an air classifier. Recently, it has been proposed that there exist

also pseudo active sites (Dickhoff et al., 2005b). These are the smooth carrier planes that are well accessible to the press-on forces during mixing. Adhesive forces between drug and carrier particles on these crystal planes may be increased compared to those for drug particles on similar planes where the press-on forces are not effective. However, the increase may not be so extreme as to achieve the magnitude of the adhesive forces with which drug particles are attached to 'real active carrier sites'. The relevance of these pseudo active sites seems furthermore confined to low carrier payloads. At high payloads (when multi-layers of drug particles around the carrier crystals exist), the press-on forces are rather effective over the entire carrier surface.

The relevance of inertial and frictional press-on forces during mixing is not confined to increasing the adhesive forces in the mixture. These forces are also responsible for drug particle agglomeration on the carrier surface (Kulvanich and Stewart, 1987; de Boer et al., 2004b), or the agglomeration of drug and fine lactose particles (Podczeck, 1998). Drug (and lactose) particle agglomeration increases the magnitude of the removal forces acting on such particles during inhalation, which leads to a higher fraction of drug detached (Louey and Stewart, 2002). If such particles can be further de-agglomerated before they leave the inhaler (classifier), they may contribute to a high fine particle fraction (fpf) (de Boer et al., 2004a/b). But if detached drug agglomerates are strong enough to withstand the forces that need to break them up, the fraction detached may be high, but fpf will be unsatisfactory (Podczeck, 1998). This may also be the case for drug agglomerates that have their origin in the starting material. Such agglomerates are broken up by the frictional and inertial press-on forces during mixing (de Boer et al., 2004b), unless the mixing time is too short or the press-on forces in the powder during mixing are not high enough (as for small carriers). Next to the carrier size fraction (powder bulk properties), the magnitude of these forces is determined by the type of mixer used, the batch size and the mixing time.

Finally, it is very important to recognise that some of the parameters mentioned above may have different implications under different circumstances, and that interactions between them exist, which has been mentioned only in a few studies before (Zeng et al., 2001a; Flament et al., 2004).

3.5. Estimating the drug storage volumes of large carrier surface discontinuities

Although the possible implications of the presence of carrier surface discontinuities are well recognised (de Boer et al., 2003a; Dickhoff et al., 2005a/b), there is a lack of adequate characterisation techniques. Surface rugosity parameters based on specific surface area measurements by permeametry (Ganderton and Kassem, 1991) or by nitrogen adsorption (de Boer et al., 2003b), and surface roughness expressions based on particle perimeter-diameter ratios (e.g. Kawashima et al., 1998; Zeng et al., 2000), are not sufficiently discriminating between different types of carrier surface irregularities. More detailed information can be obtained from laser profilometry (Podczeck, 1998) or atomic force microscopy (Price et al., 2002), but these techniques provide only information of small areas and are not suitable for mapping total, nor extreme topographies. Recently, more sophisticated image analysis software has become available (e.g. Flament et al., 2004). Such techniques might make it possible to estimate more precisely the surface area over which large carrier discontinuities exist. Visual observation has always been the most direct way to gain information. It only requires development of appropriate methods to qualify and quantify this information.

From careful observation of a great number of carrier fractions with scanning electron microscopy (SEM), it can be concluded that the mean depth of carrier surface depressions and

projections varies more or less proportionally with the size of the carrier particles. This is not unexpected, because discontinuities (after being originated, mostly as a local distortion of the crystal lattice) grow with the same speed as the crystals. This is shown in Fig. 8.4 for particles of size fractions 45-63 and 150-200 µm. Different magnifications were applied to depict the particles equally large. Both micrographs suggest that the fraction of the carrier surface over which these discontinuities exist, is more or less the same too. So, the volume (V_{CSD} in m^3 per gram carrier) of the surface discontinuities may be largely independent of the carrier particle diameter for products of the same type.

This idea is supported by Fig. 8.2, showing that the maximum, or plateau value for the percent dislodged is achieved at approximately the same carrier payload for all carrier fractions used. Apparently, a reduction in mean pore depth with decreasing carrier diameter is compensated largely by an increase in the specific surface area. This can be derived mathematically. If the mean pore depth (H) is a constant fraction (X) of the carrier diameter (D), H may be written as H = X.D. Similarly, the carrier surface (A) over which the discontinuities exist, may be determined by a surface fraction (Y): $A = Y.6D^{-1}.\rho^{-1}$, where ρ is the true density of lactose. Multiplication of H and A yields the pore volume (V_{CSD}), which (after re-arrangement of terms) becomes:

$$V_{CSD} = 6X.Y.\rho^{-1} \ (m^3/g). \qquad [8.1]$$

In this expression the diameter (D) has been eliminated.

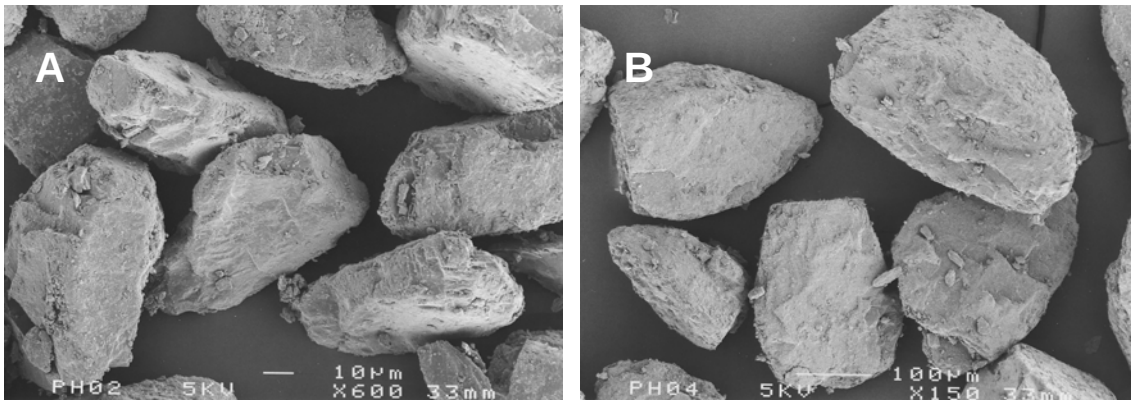

Figure 8.4. SEM micrographs of carrier size fractions 45-63 µm (A) and 150-200 µm (B) from Pharmatose 150 M at different magnifications (600 and 150 x respectively) depicting the carrier particles equally large.

From the saturation concentrations in Table 8.2, V_{CSD} can be assessed. For example, the saturation concentration for the coarse carrier fraction of 250-355 µm in this study is 0.775 g per square meter of carrier surface. From the calculated specific surface area of this carrier fraction (0.0129 m^2/g), it can be computed that this concentration equals 0.01 g drug per gram carrier. Estimating (on the basis of known porosities of soft spherical pellets) that the powder porosity (ε) for the drug in the carrier surface discontinuities (at 1% payload) is approximately 0.6, the apparent density ($\rho_S = \rho_0(1-\varepsilon)$) of this powder becomes 0.496×10^6 g/m^3 (the true density, ρ_0, of budesonide being 1.240×10^6 g/m^3). So, the amount of drug in

the carrier surface discontinuities in the saturation situation (0.01 g) has a volume of approximately 0.02 x 10^{-6} m^3 (per gram carrier).

If V_{CSD} equals 0.02 x 10^{-6} m^3/g carrier, and the true density of lactose is 1.54 x 10^{-6} g/m^3, the product of X and Y in Eq. 8.1 has a value of 0.005. From SEM micrographs it can be concluded that the surface area over which the large discontinuities exist, is approximately 10% of total carrier surface area. So, the Y-factor is 0.1 and the diameter fraction X defining the mean pore depth becomes 0.05. With this X-factor, the actual (mean) pore depth as function of the (mean) carrier diameter can be assessed (Table 8.4). Table 8.4 also presents pore depths for other values of the Y-factor, as well as for other powder porosities in the carrier surface discontinuities. The calculations may be arguable, because X, Y and ε have not actually been measured yet, but Table 8.4 shows that for a wide range of plausible values for these parameters, there exist carrier particles with mean pore depths that are smaller than the diameter of adhering drug particles (for a typical inhalation drug X_{50} ≈ 1.5 µm and X_{90} ≈ 3.5 µm). This may be the case for carrier diameters up to 125 µm, which includes most carrier fractions used in marketed products and in various studies.

Table 8.4. Mean depth of carrier surface discontinuities (in µm) as function of carrier diameter derived from the saturation concentrations of these discontinuities (Fig. 8.2) and Equation 8.1. ε is the powder porosity in the discontinuities; X is the carrier diameter fraction determining the mean pore depth and Y is the carrier surface fraction determining the surface over which the discontinuities extend. See the text for further explanation and calculations. Depths marked with * are less than the X_{90}-value of a typical inhalation drug; depths marked with ** are less than the X_{50}-value.

ε	Y	X	Carrier diameter (µm)				
			250	125	60	30	15
0.6	0.05	0.103	25.8	12.9	6.2	3.1*	1.6*
0.6	0.10	0.052	13.0	6.5	3.1*	1.6*	0.8**
0.6	0.20	0.026	6.5	3.3*	1.6*	0.8**	0.4**
0.45	0.10	0.038	9.4	4.7	2.3*	1.1**	0.6**
0.75	0.10	0.082	20.7	10.3	5.0	2.5*	1.2**

There are several wide-ranging consequences of this recognition for the mixing and inhalation processes. It is beyond the scope of this study to discuss these consequences in detail, but press-on forces may get better hold of drug particles during mixing, drug agglomerates on the carrier surface may become smaller, drug distribution over the carrier surface (including the active sites) may improve, and the effectiveness of various types of detachment forces during inhalation may increase when the carrier size is decreased towards diameters for which the mean pore depth is smaller than the (median) drug particle diameter.

3.6. Modelling of the saturation of active sites

The finding that saturation of the large surface cavities is completed at a much lower payload (% w/w) than saturation of the active sites (Table 8.2) seems to suggest that a substantial part of the active sites is outside the large surface discontinuities inside which drug particles are wiped together. It could also be however, that the active sites are inside the discontinuities and become first saturated when the drug particles are effectively brought into contact with these sites, for instance by powder densification (particle re-arrangement) in the pores as a result of the action of the press-on forces at higher carrier payloads. The relatively strong fall off for the increase rate in percent dislodged (Fig. 8.2) starting already at payloads of 0.2% (w/w), points in this direction. Also the finding that the degree of saturation of the active sites is not simply proportional with the number of drug particles on the carrier surface,

suggests that the active sites are inside the large carrier surface clefts and pores. Support is obtained from Fig. 8.5, in which computed and experimental values for percent dislodged (for a coarse carrier fraction of 250-355 µm) as function of carrier surface payload are presented for different saturation kinetics, assuming that (at 60 l/min) only particles attached to the active sites are not detached (see materials and methods for the calculations). The figure shows that the experimental data obtained at 60 l/min fairly well match the theoretical curve for an exponential (square root) increase in the degree of saturation of the active sites. An initially high degree of occupation (at low payload) is followed by a much slower occupation rate at higher payloads. The high degree of occupation of the active sites at low payloads may be explained with effective relocation of drug particles from sites with lower binding force to active sites (of which there is a relative excess at low payload). At higher payloads, when large particle associations (with a high porosity) start to fill up the carrier surface discontinuities, the relocation process is likely to slow down (as confirmed by Fig. 8.3). Only by particle re-arrangement in the pores (powder densification), further saturation of the active sites inside these discontinuities is possible. This could explain why it takes a multilayer of drug around a coarse carrier fraction (250-355 µm) to obtain complete saturation of the active sites (In Table 8.2 CC, for the coarse fraction is 354%). There is support for this supposition from the fact that such active sites are frequently spots with relatively high amounts of impurities (e.g. salts, protein and peptide residues). They origin from the mother liquor which concentrates particularly in the carrier surface irregularities when the wet crystals are transferred to the driers. The disproportional part of the drug being immobilised on the active sites at low carrier payloads (< 0.2%) explains why low payloads are disadvantageous in respect of drug redispersion.

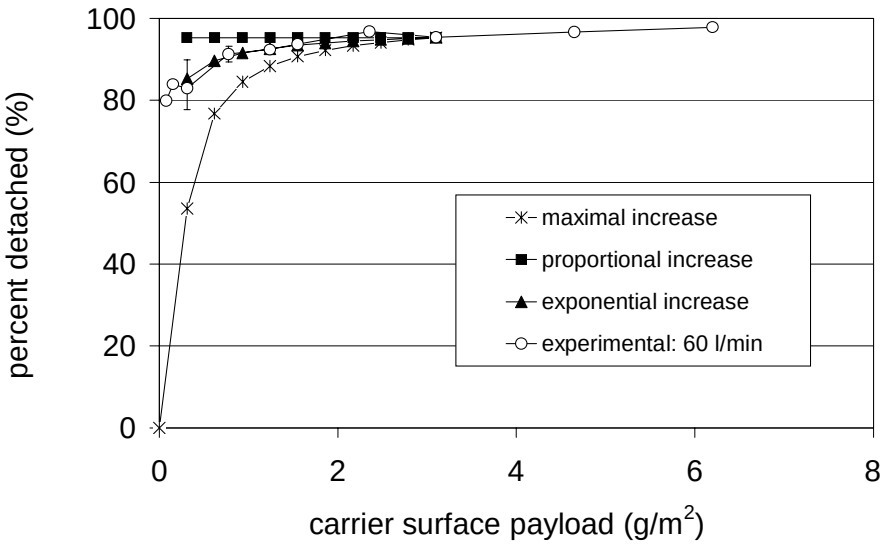

Figure 8.5. Comparison of experimentally obtained (at 60 l/min) and computed percent of drug detached from carrier fraction 250-355 µm as function of the carrier surface payload. Conditions and calculations are given in the section materials and methods.

4. Conclusions

At least three different carrier properties are relevant to drug-to-carrier interaction in adhesive mixtures and drug detachment during inhalation. Next to the drug binding capacity

of the active carrier sites (in g/m^2) and the volume of large surface discontinuities (in m^3/g), the carrier bulk properties are important. The relative importance of each of these properties depends on the carrier payload, the mixing intensity and time and the type (and size) of separation forces generated during inhalation. At low payload, and in the presence of large carrier surface discontinuities, the influence of bulk properties may be small. At higher payloads, the effect of the active sites on drug redispersion is of lower importance. When inertial separation forces are generated, large surface discontinuities may be beneficial, as they provide shelter from press-on forces during mixing which increase the interparticulate forces. When on the other hand de-agglomeration relies on frictional, drag and lift forces, large surface projections and depressions also provide shelter from these separation forces. It has been found that saturation of the active sites occurs at much higher carrier payloads than that of the large surface discontinuities. It has also been calculated that the degree of saturation of the active sites increases exponentially (according to a square root function) with the carrier payload, which could be the result of powder densification in the large surface discontinuities.

Finally, there are good reasons to believe that the volume of the large surface discontinuities is more or less independent of the carrier diameter for carrier fractions from the same type of lactose. A reduction in depth of these discontinuities with decreasing carrier diameter is compensated by an increase in surface area over which these cavities exist. For fine carriers the depth of surface discontinuities may be smaller than the size of adhering drug particles. As a result, mixtures with fine and coarse carriers may behave rather differently during mixing and inhalation, particularly with respect of the effectiveness of press-on and detachment forces.

Acknowledgement

The authors would like to thank Mrs. Beekhuis for carefully screening the manuscript.

References

de Boer, A.H., Hagedoorn, P., Gjaltema, D., Goede, J., Frijlink, H.W., 2003a. Air classifier technology (ACT) in dry powder inhalation Part 1. Introduction of a novel force distribution concept (FDC) explaining the performance of a basic air classifier on adhesive mixtures. Int. J. Pharm. 260, 187-200.

de Boer, A.H., Hagedoorn, P., Gjaltema, D., Goede, J., Kussendrager, K.D., Frijlink, H.W., 2003b. Air classifier technology (ACT) in dry powder inhalation Part 2. The effect of lactose carrier surface properties on the drug-to-carrier interaction in adhesive mixtures for inhalation. Int. J. Pharm. 260, 210-216.

de Boer, A.H., Hagedoorn, P., Gjaltema, D., Lambregts, D., Irngartinger, M., Frijlink, H.W., 2004a. The rate of drug particle detachment from carrier crystals in an air classifier based inhaler. Pharm Res. 21, 2158-2166..

de Boer, A.H., Hagedoorn, P., Gjaltema, D., Lambregts, D., Irngartinger, M., Frijlink, H.W., 2004b. The mode of drug particle detachment from carrier crystals in an air classifier based inhaler. Pharm. Res. 21, 2167-2174.

Buckton, G., 1997. Characterisation of small changes in the physical properties of powders of significance for dry powder inhaler formulations. Adv. Drug. Del. Rev. 26, 17-27.

Dickhoff, B.H.J., de Boer, A.H., Lambregts, D., Frijlink, H.W., 2003. The effect of carrier surface and bulk properties on drug particle detachment from crystalline lactose carrier particles during inhalation, as function of carrier payload and mixing time. Eur. J. Pharm. Biopharm. 56, 291-302.

Dickhoff, B.H.J., de Boer, A.H., Lambregts, D., Frijlink, H.W., 2005a. The interaction between carrier rugosity and carrier payload, and its effect on drug particle redispersion from adhesive mixtures during inhalation. Eur. J. Pharm. Biopharm. 59, 197-205.

Dickhoff, B.H.J., de Boer, A.H., Lambregts, D., Frijlink, H.W., 2005b. Drug particle detachment from carrier crystals during inhalation in dependence of carrier size, type of carrier rugosity, carrier payload and mixing intensity. Submitted to Int. J. Pharm.

Flament, M-P., Leterme, P., Gayot, A., 2004. The influence of carrier roughness on adhesion, content uniformity and the in vitro deposition of terbutaline sulphate from dry powder inhalers. Int. J. Pharm. 275, 201-209.

Ganderton, D., Kassem, N.M., 1991. Aerosol carriers. WO 91/11179.

Iida, K., Hayakawa, Y., Okamoto, H., Danjo, K., Leuenberger, H., 2003. Preparation of dry powder inhalation by surface treatment of lactose carrier particles. Chem. Pharm. Bull. 51, 1-5.

Kawashima, Y., Serigano, T., Hino, T., Yamamoto, H., Takeuchi, H., 1998. Effect of surface morphology of carrier lactose on dry powder inhalation property of pranlukast hydrate. Int. J. Pharm. 172, 179-188.

Kulvanich, P., Stewart, P.J., 1987. The effect of particle size and concentration on the adhesive characteristics of a model drug-carrier interactive system. J. Pharm. Pharmacol. 39, 673-678.

Larhrib, H., Zeng, X.M., Martin, G.P., Marriott, C., Pritchard, J., 1999. The use of different grades of lactose as a carrier for aerosolised salbutamol sulphate. Int. J. Pharm. 191, 1-14.

Louey, M.D., Stewart, P.J., 2002. Particle interactions involved in aerosol dispersion of ternary interactive mixtures. Pharm. Res. 19, 1524-1531.

Newhouse, M.T., Hirst, P.H., Duddu, S.P., Walter, Y.H., Tarara T.E., Clark, A.R., Weers, J.G., 2003. Inhalation of a dry powder Tobramycin Pulmosphere formulation in healthy volunteers. Chest 124, 360-366.

Podczeck, F., 1998. The relationship between physical properties of lactose monohydrate and the aerodynamic behaviour of adhered drug particles. Int. J. Pharm. 160, 119-130.

Price, R., Young, P.M., Edge, S., Staniforth, J.N., 2002. The influence of relative humidity on particulate interactions in carrier-based dry powder inhaler formulations. Int. J. Pharm. 246, 47-59.

Schlimmer, P., 2002. Single-dose comparison of formoterol (Oxis) Turbuhaler 6 microg and formoterol Aerolizer 12 microg in moderate severe asthma: a randomised, crossover study. Pulm. Pharmacol. Therapy 15, 369-374.

Staniforth, J.N., 1995. Improvements in and relating to carrier particles for use in dry powder inhalers. WO 95/11666.

Staniforth, J.N., 1996. Carrier particles for use in dry powder inhalers. WO 96/23485.

Zeng, X-M., Martin, G.P., Marriott, C., Pritchard, J., 2000. The influence of carrier morphology on drug delivery by dry powder inhalers. Int. J. Pharm. 200, 93-106.

Zeng, X-M., Martin, G.P., Marriott, C., Pritchard, J., 2001a. Lactose as a carrier in dry powder formulations: the influence of surface characteristics on drug delivery. J. Pharm. Sci. 90, 1424-1434.

Zeng, X-M., Martin, G.P., Marriott, C., Pritchard, J., 2001b. The use of lactose recrystallised from carbopol gels as a carrier for aerosolised salbutamol sulphate. Eur. J. Pharm. Biopharm. 51, 55-62.